Available online at www.sciencedirect.com
SCIENCE DIRECT®
Materials Chemistry and Physics 94 (2005) 131–140
MATERIALS CHEMISTRY AND PHYSICS
www.elsevier.com/locate/matchemphys

The study of vacuum-furnace brazing of C103 and Ti–6Al–4V using Ti–15Cu–15Ni foil

In-Ting Hong, Chun-Hao Koo *

Department of Materials Science and Engineering, National Taiwan University, Taipei, Taiwan, ROC

Received 15 November 2004; received in revised form 1 April 2005; accepted 19 April 2005

Abstract

C103 and Ti–6Al–4V alloys jointed with Ti–15Cu–15Ni (wt.%) commercial brazing foil by vacuum-furnace brazing were investigated. Our previous study [I.-T. Hong, C.-H. Koo, Mater. Sci. Eng. A 398 (2005) 113] demonstrated that Ti–15Cu–15Ni (wt.%) filler-metal can successfully braze C103 and Ti–6Al–4V alloys, and identified all phases in the joint interface. The relationship between the microstructure and the joint performance, and the solidification process of the liquid filler-metal in the joint interface were also studied in detail. Therefore, the current study mainly focuses on how to further improve the microstructure and mechanical properties of the C103/TiCuNi/Ti–6Al–4V joint via post-brazing treatments or using various joint designs, such as overlap-length of joints, surface roughness of the parent-metals and joint clearance. Moreover, the high temperature shear strength of the C103/TiCuNi/Ti–6Al–4V joint was investigated to evaluate its limit service temperature. The experimental results reveal that the fracture load of joint reaches a maximum of 31,076 N, and the joint fractures in C103 parent-metal when the overlap-length of the joint increases to 3.5 times the thickness of the parent-metal (3.5*T*, 7 mm). However, the joint shear strength decreases with the overlap-length of the joint because of the non-uniform stress distribution in the lap joint during shear test. Post-brazing treatment at 880 °C for 4 h increases the shear strength of the joint brazed at 960 °C for 15 min by 16%, from 352 to 411 MPa. However, prolonging the post-brazing time to 6 h reduces the shear strength of the joint to 299 MPa. A comparison with the coarse Widmanstätten structure reveals that the presence of some fine Widmanstätten structure that forms in the joint interface during post-brazing treatment does not seem to deteriorate the joint shear strength. Moreover, the shear strength of joints decreases as the surface roughness of parent-metals decreases or the joint clearance increases. The results of the high temperature shear test reveal that the shear strength of the C103/TiCuNi/Ti–6Al–4V joint maintains at around 300 MPa at the test temperature below 600 °C. However, as the test temperature exceeds 600 °C, the shear strength of C103/TiCuNi/Ti–6Al–4V joint declines greatly.

Keywords: Ti–6Al–4V; C103; TiCuNi filler-metal; Shear strength; Vacuum-furnace brazing

1. Introduction

The element columbium was discovered and identified in 1801. It was until 1844 that the niobium was firstly separated from columbium by a German scientist. Niobium is a refractory metal with a high melting point of 2468 °C and a relatively low density of 8.57 g cm^{-3} [1]. Niobium alloys are widely applied for rocket and aerospace applications, because niobium has low density and excellent strength at elevated-temperature. One specific Nb alloy, C103 [Nb–10Hf–1Ti (wt.%)], exhibits superior strength at elevated-temperature, and is less susceptible to recrystallization and softening than pure niobium. Therefore, C103 is one of the most important niobium alloys for use in rocket and missile applications [1,2,5].

Ti–6Al–4V alloy, an α–β Ti alloy which can be strengthened by solutioning and aging heat treatments, is the most important and widely used titanium alloy [1]. Ti–6Al–4V alloys are used in a wide range of areas, including daily life, aviation and nuclear industry, and particularly in the aerospace and defense industries [3].

Rocket-propulsion systems or missile combustion chambers may contain C103 refractory metal and Ti–6Al–4V alloy. Practical rocket and missile applications depend on joining

* Corresponding author. Tel.: +886 2 2363 4097; fax: +886 2 2363 4562.
E-mail addresses: bcc22@ms53.hinet.net (I.-T. Hong), chkoo@ccms.ntu.edu.tw (C.-H. Koo).

0254-0584/$ – see front matter © 2005 Elsevier B.V. All rights reserved.
doi:10.1016/j.matchemphys.2005.04.021

two dissimilar alloys, C103 and Ti–6Al–4V. Therefore, technologies for joining C103 and Ti–6Al–4V alloys are very important for the production of rocket-propulsion systems or missile combustion chambers [1–3].

So far, only limited data are available on refractory metal and titanium alloy joints brazed with some filler-metals [8,9,14,15]. The microstructures of Nb/Ti alloy joints and their phase identifications have not been studied thoroughly in detail. Previous investigation [23,24] proved that C103 and Ti–6Al–4V alloys can be successfully brazed using Ti–15Cu–15Ni (wt.%) filler-metal foil. Therefore, this study focuses on how to further improve the microstructure and mechanical properties of the C103/TiCuNi/Ti–6Al–4V brazed joint through various joint designs and post-brazing treatments. Several brazing conditions and factors, such as post-brazing treatment, overlap-length, the surface roughness of parent-metals, joint clearance and the high temperature shear strength of the C103/TiCuNi/Ti–6Al–4V joints, are comprehensively investigated to elucidate the effect of these brazing conditions and factors on the microstructure and mechanical properties of joints. The failure mode of the C103/TiCuNi/Ti–6Al–4V joint is also studied to realize the relationships between the crack propagation and the shear strength of the joints.

2. Experimental procedures

The parent-metals used in this work are the sheets of C103 and Ti–6Al–4V alloys with a thickness of 2 mm. Both alloy sheets were cut into 10 mm × 10 mm × 2 mm (for microstructural analysis) or 15 mm × 12 mm × 2 mm (for shear strength testing) by wire-cutting for brazed joining. These specimens were then polished by wet SiC paper, and subsequently were ultrasonically cleaned by acetone before brazing. A brazing foil of Ti–15Cu–15Ni (wt.%) was chosen as the filler-metal, with the size of 60 μm in thickness and 50 mm wide. This clad Ti–15Cu–15Ni material is a three-layered sandwich-like strip, in which Ti and the Cu–Ni alloys are widely separated, and has liquidus temperatures around 960 °C. The brazing foil was cleaned in acetone before brazing. The filler-metal is sandwiched between two parent-metals fixed with a stainless steel clamp, and then this sandwiched brazement was carefully placed into a vacuum furnace. Furnace brazing was performed in a vacuum of 1×10^{-6} Torr. The specimens were prepared and treated in several ways to produce the test specimens with different conditions for various investigations. Table 1 lists the details of various investigations for each specimen. After brazing, all the specimens were furnace-cooled to room temperature. Following bonding, specimens were cut by a low speed diamond saw, mounted and polished. The cross-section of the brazed specimens was examined by a Phillip XL-30 scanning electron microscope (SEM) with an accelerating voltage of 20 kV. Quantitative chemical analysis was conducted by a JEOL JXA-8800M electron probe microanalyzer (EPMA) equipped with a wavelength dispersive spectrometer (WDS), operating with the operation voltage of 20 kV and the spot size of 1 μm. Shear tests were conducted at 25–800 °C in a Shimadzu AG-10 universal testing machine equipped with a furnace at a constant speed of 1 mm/min.

3. Results and discussion

3.1. The microstructural analysis of the C103/TiCuNi/Ti–6Al–4V joint brazed at 960 °C

Fig. 1 displays the SEM backscattered electron images (BEIs) of the C103/TiCuNi/Ti–6Al–4V joint brazed at 960 °C for 5 min and the line scan profile (LSP) curves of joint interface. The LSP curves show that the contents of Nb, Ni, Cu and Ti change with the location of joint interface, causing the different microstructure in joint interface. Additionally, the EPMA chemical analyses of seven characteristic zones are also listed in Fig. 1. According to the microstructural morphology, the microstructure in joint interface can be divided into seven characteristic zones, described as follows.

Zones I and VII are the C103 and Ti–6Al–4V parent-metals, respectively. Zone II is the reaction area of the C103

Table 1
Summary of brazing conditions used in the experiment

	Brazing condition	Overlap-length (T = 2 mm)	Joint clearance (μm)	Surface roughness (the grit of SiC paper)	Shear test temperature (°C)
Overlap-length investigation	960 °C, 15 min	1T, 2T, 3T, 3.5T, 4T	60	100	25
Investigation of post-brazing treatment	960 °C, 15 min and then heated at 880 °C for 2, 4 and 6 h	1T	60	100	25
Investigation of surface roughness	960 °C, 15 min	1T	60	40, 100, 600, 1200	25
Investigation of joint clearance	960 °C, 15 min	1T	60, 120, 180, 240	100	25
Investigation of high temperature shear strength	960 °C, 15 min	1T	60	100	25, 200, 400, 600, 700, 800

(a)

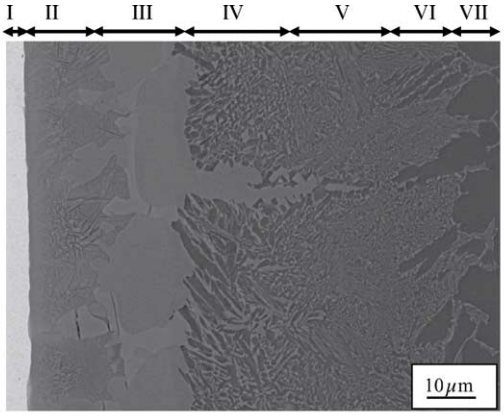

(b)

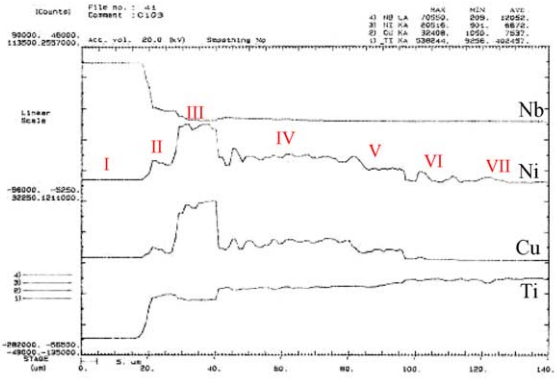

(c)

Element (wt.%)	Ti	Cu	Ni	Nb	Hf	Al	V
Zone I	**1.0**	**0.0**	**0.0**	**89.1**	**9.9**	**0.0**	**0.0**
Zone II	64.4	2.7	2.6	28.3	2.0	0.0	0.0
Zone III	63.6	22.1	13.9	0.4	0.0	0.0	0.0
Zone IV	84.8	7.9	6.7	0.1	0.0	0.4	0.2
Zone V	87.7	6.4	5.1	0.0	0.0	0.6	0.2
Zone VI	**86.4**	**2.3**	**1.9**	**0.0**	**0.0**	**5.7**	**3.7**
Zone VII	**89.7**	**0.0**	**0.0**	**0.0**	**0.0**	**6.1**	**4.2**

Fig. 1. (a) The microstructure of C103/TiCuNi/Ti–6Al–4V joint brazed at 960 °C for 5 min, showing the seven zones of different phases in joint interface. (b) The line scan profile (LSP) curves of Nb, Ni, Cu and Ti elements. (c) The EPMA analyses of the seven characteristic zones.

parent-metal with the molten filler-metal. During brazing, the dissolved elements of C103 parent-metal react with molten filler-metal in this layer, which is a mixed region of three phases consisting of the Ti-rich phase, the Nb-rich phase and acicular intermetallic phase, such as Ti_2(Ni, Cu) and/or Ti_2(Cu, Ni).

Zone III is the continuous intermetallic-layer, which is mainly comprised of Ti_2(Ni, Cu) and/or Ti_2(Cu, Ni) intermetallic phases [24]. Because of the segregation occurred during isothermal solidification, zone III contains higher Cu and Ni concentration than the original filler-metal.

Zones IV and V are the hypoeutectic and hypereutectoid structure, respectively. The composition of the TiCuNi filler-metal is close to that of the Ti–Cu–Ni ternary eutectic point [7]. With the diffusion of molten filler-metal and the dilution of parent-metals, the composition of the molten filler-metal deviates from eutectic to hypoeutectic and/or hypereutectoid [24], as depicted by paths 1 and 3 in Fig. 2. Therefore, the joint interface mainly consists of hypoeutectic and/or hypereutectoid structure, marked by IV and V in Fig. 1. Additionally, during brazing, the diffusion of alloying elements from parent-metals into liquid filler-metal is preferable than that from liquid filler-metal into parent-metals because the diffusivity of elements in molten state is much higher than that in solid state [16–18,21]. Therefore, for zones IV and V, the dilution of parent-metals might be the dominating mechanism in this brazing system.

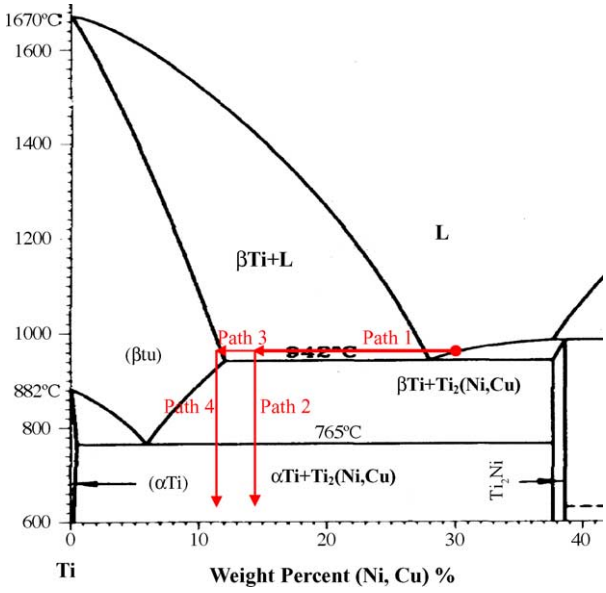

Fig. 2. The pseudo Ti–(Ni, Cu) binary phase diagram. There are four types of phase-transformation path produced by isothermal diffusion and dilution of parent-metals (Paths 1 and 3), and cooling (Paths 2 and 4). The filled circle denotes the composition of original filler-metal [6].

Zone VI is the acicular Widmanstätten structure area. During brazing, the Cu and Ni atoms in filler-metal diffuse into the front of the Ti–6Al–4V parent-metal, as shown in Fig. 1(b), and reduce its β-transus temperature. Therefore, the α-Ti matrix, wherein the Cu and Ni atoms diffuse, transforms into the β phase during brazing. On cooling, the β phase transforms back into the α phase and forms the acicular Widmanstätten structure [19,20].

3.2. Room temperature and high temperature shear testing of the C103/TiCuNi/Ti–6Al–4V joint

Fig. 3 shows the room temperature shear strength of the C103/TiCuNi/Ti–6Al–4V joint brazed at 960 °C for 5–20 min. As a result, the shear strength of the joint brazed at 960 °C for 5 min is insufficient because the continuous intermetallic-layer consisting of large amounts of intermetallics remains in the central region of joint interface, as shown in Fig. 4(a). As the brazing time is prolonged to 15 min, the continuous intermetallic-layer disappears and is displaced by the hypoeutectic and hypoeutectoid structure, as shown in Fig. 4(c). The maximum shear strength of

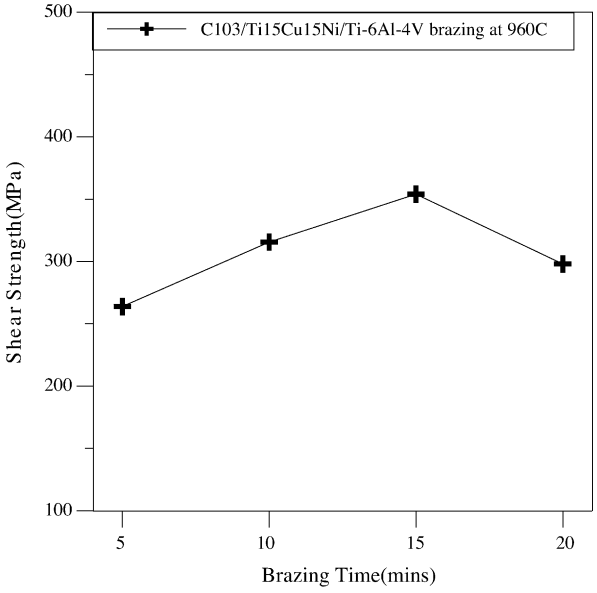

Brazing conditions	960 °C 5mins	960 °C 10mins	960 °C 15mins	960 °C 20mins
Fracture mode	I	I	II	II
Shear strength (MPa)	263	315	354	298

Fig. 3. The shear strength of the C103/TiCuNI/Ti–6Al–4V joint brazed at 960 °C for various brazing times.

354 MPa is achieved. However, further prolonging the brazing time to 20 min causes the formation of coarse acicular Widmanstätten structure in front of Ti–6Al–4V parent-metal, as shown in Fig. 4(d), and reduces the shear strength to 298 MPa. According to the observations of fracture surface, the specimens brazed at 960 °C for 5 or 10 min are fractured in the continuous intermetallic-layer, and such a failure mode is denoted as mode I in this study. When the brazing time is prolonged to 15 or 20 min, the specimens are fractured near the joint interface between the C103 parent-metal and C103 reaction area, and the failure mode of the joint changes from mode I to mode II. Three kinds of failure modes of the C103/TiCuNi/Ti–6Al–4V joint can be observed in the fracture surface of all specimens and are discussed in Section 3.3. In addition, for mechanical prospect of the C103/TiCuNi/Ti–6Al–4V joint, brazing at 960 °C for 15 min is the optimized condition to achieve the maximum shear strength [24]. Therefore, specimens used in the other investigations in this study are also brazed under the same condition.

Fig. 5 shows the high temperature shear strength of the C103/TiCuNi/Ti–6Al–4V joint, indicating that the shear strength of the C103/TiCuNi/Ti–6Al–4V joint can be maintained around 300 MPa at a temperature below 600 °C. However, the joint shear strength declines significantly as the temperature exceeds 600 °C. Accordingly, the limit service temperature of the C103/TiCuNi/Ti–6Al–4V joint is below 700 °C. Exceeding the limit service temperature causes the joints to failure under low loading.

3.3. Overlap-length investigation of the C103/TiCuNi/Ti–6Al–4V joint

The shear strength or tensile strength of the brazed joint depends mainly on its overlap-length. Too small an overlap-length causes the brazed joint to fail below the required

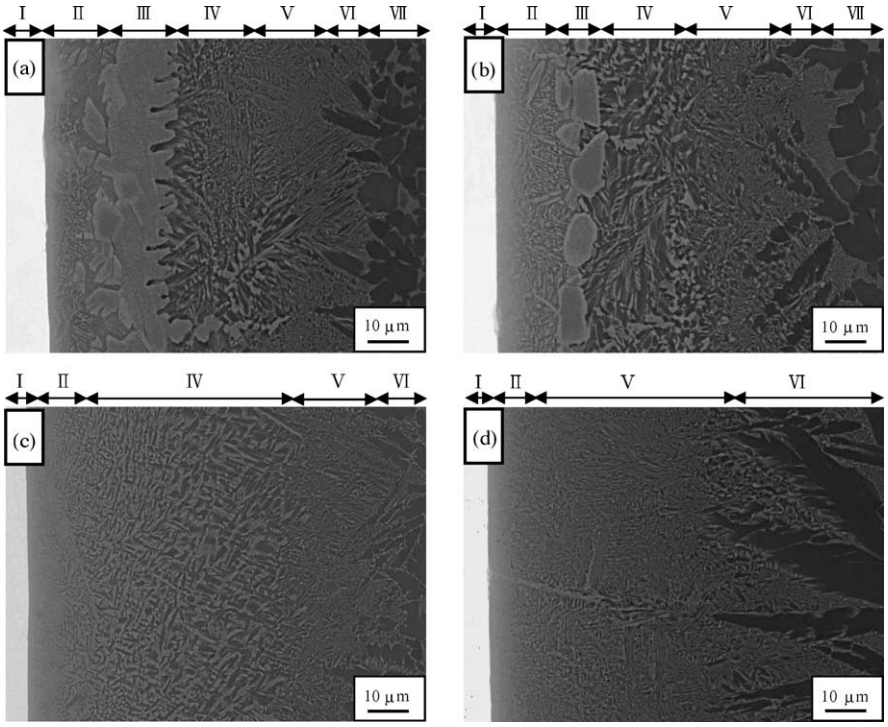

Fig. 4. The back-scattering electron images (BEIs) of C103/TiCuNi/Ti6Al4V specimens brazed at 960 °C for: (a) 5 min, (b) 10 min, (c) 15 min and (d) 20 min.

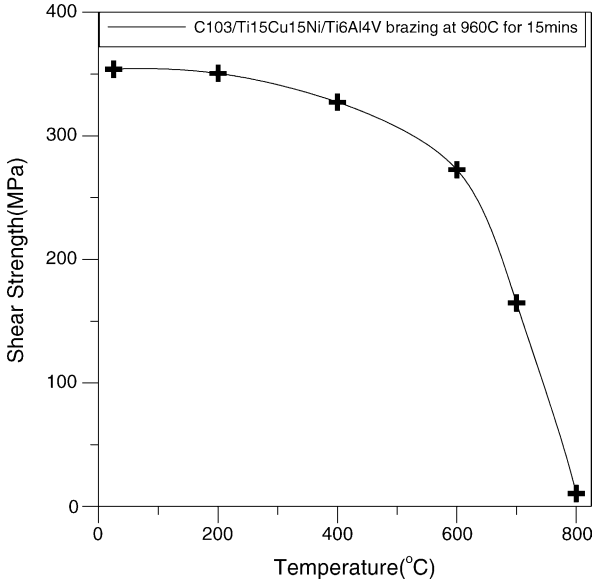

Fig. 5. The high temperature shear strength of the C103/TiCuNi/Ti–6Al–4V joint brazed at 960 °C for 15 min.

loading, whereas too large an overlap-length means an unnecessarily wasteful material. Generally, the brazed joint with an overlap-length of three to five times the thickness of the parent-metals can achieve the maximum load-bearing capacity [4]. However, a large number of tests must be conducted to optimize the overlap-length for a specific brazed joint.

Fig. 6 is the correlation diagram between the fracture load, shear strength and the overlap-length of the brazed joint. The fracture load of the joint with an overlap-length of 2 mm, which is one time the thickness of parent-metal, is as low as 10,613 N, because of its short overlap-length. The load-bearing capacity of the brazed joint generally increases

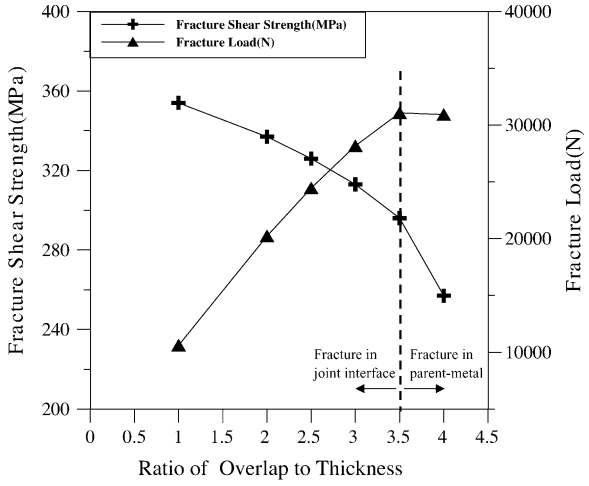

Over lap distance	1T	2T	2. 5T	3T	3. 5T	4T
Fracture Load (N)	10613	20217	24451	28165	31076	30920
Fracture Shear strength (MPa)	354	337	326	313	296	257

Fig. 6. Correlation diagram between shear strength and overlap distance of the C103/TiCuNi/Ti–6Al–4V joint brazed at 960 °C for 15 min.

with the overlap-length or overlap area. As a result, the fracture load of the joint rises to 28,165 N as its overlap-length increases to three times the thickness of the parent-metal (3*T*, 6 mm). Further increasing the overlap-length to 3.5 times the thickness of the parent-metal (3.5*T*, 7 mm) raises the fracture load to as high as 31,076 N, and the brazed joint fractures in C103 parent-metal. In Fig. 6, the point of intersection between the horizontal line and the oblique line is the critical overlap-length of the joint, and this value is about 3.2.

Additionally, the fracture shear strength for each overlap-length was calculated as the failure load divided by the overlap area, as shown in Fig. 6. The trend of the shear strength reduction with the increase of the overlap-length is different from that of the fracture load. This phenomenon had been discussed in some references [25–28], in which the Von Mises stress was utilized to demonstrate the decreasing of the joint shear strength. As the overlap-length of joint increases, the Von Mises stress distribution becomes less and less uniform. The middle portion of the overlap contributes less and less to the overall load-carrying capacity of the joint, whereas the ends of the joint become “overloaded”. The non-uniform stress distribution in the lap joint causes the decreasing of the shear strength [26,27].

Observations of all fracture surfaces reveal that the failure modes of joints can be divided into three types, based on the crack propagation of the fracture surface. These failure modes depend not only on the phase appeared in the joint interface, but also on the joint designs, such as the overlap-length or the joint clearance. In mode I, the cracks propagate along the continuous intermetallic-layer and toward the parent-metals, as shown in Fig. 7(a). When the joints are brazed at 960 °C for 5 or 10 min, the continuous intermetallic-layer remains in the joint interface, and the joints are fractured in this mode. In mode II, the cracks are initiated in C103 parent-metal and then transferred through the interface into the C103 reaction area, as shown in Fig. 7(b). When the brazing time is increased from 10 to 15 min at 960 °C, the continuous intermetallic-layer disappears so that the failure mode changes from mode I to mode II. In mode III, the cracks propagate in the joint interface and penetrate the coarse acicular Widmanstätten structure. When the brazing temperature is too high or the brazing time is too long, the coarse acicular Widmanstätten structure would be formed in the joint interface, and the joint would fracture in this mode, as shown in Fig. 7(c).

3.4. Investigation of the post-brazing treatment of the C103/TiCuNi/Ti–6Al–4V joint

A proper post-brazing treatment can improve the mechanical properties and microstructure of joints. The joints underwent post-brazing treatments at 880 °C for 2, 4 and 6 h after brazing at 960 °C for 15 min, to determine the optimized conditions for the post-brazing treatment of the C103/TiCuNi/Ti–6Al–4V joint.

In this work, the temperature of post-brazing treatment is set to 880 °C, which is far lower than the melting point of the

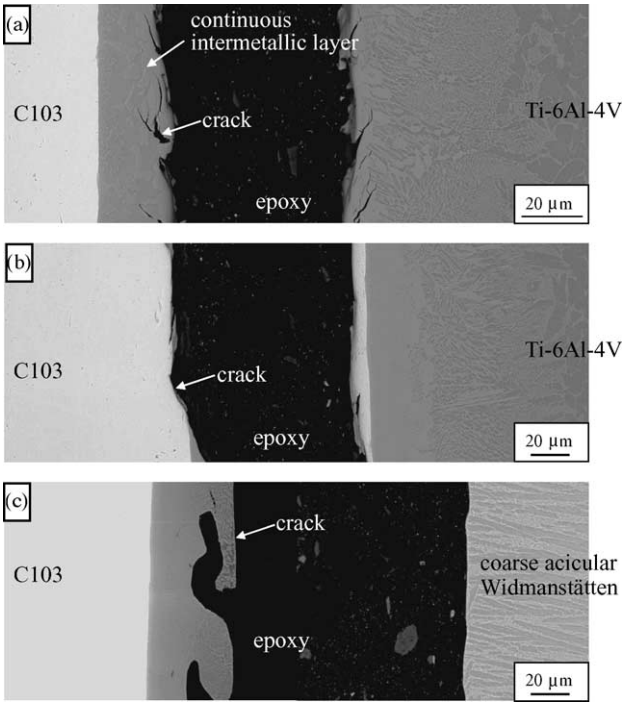

Fig. 7. Three sorts of failure mode of the C103/TiCuNi/Ti–6Al–4V joint. (a) Mode I, the cracks propagate along the residual filler-metal and toward the parent-metals. (b) Mode II, the cracks are initiated in C103 parent-metal and then transfer through the interface into the C103 reaction area. (c) Mode III, the cracks pass through the coarse acicular Widmanstätten.

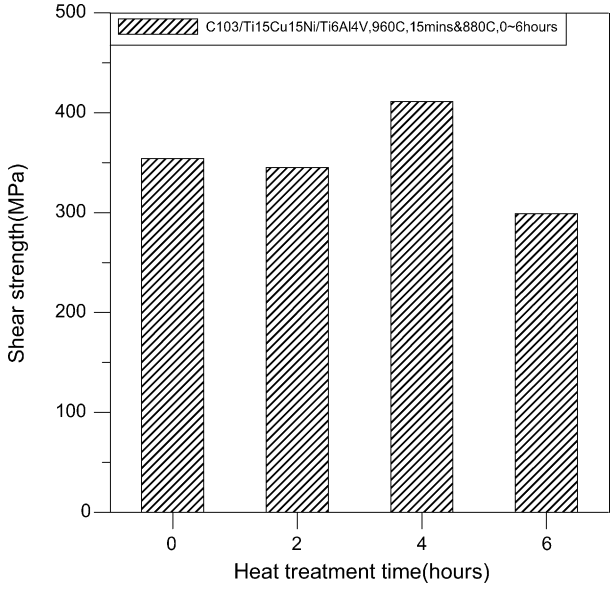

Fig. 9. The evolution of shear strength of the C103/TiCuNi/Ti–6Al–4V joint after post-brazing treatment at 880 °C for 2, 4 and 6 h, which was preceded by brazing at 960 °C for 15 min.

filler-metal and the β-transus temperature of the Ti–6Al–4V parent-metal. Therefore, during post-brazing treatment, the TiCuNi filler-metal does not remelt and the acicular Widmanstätten structure should not form in the joint interface. However, microstructural observations reveal that the acicular Widmanstätten structure is still formed in the front of Ti–6Al–4V parent-metal, as shown in Fig. 8. Although the temperature of post-brazing treatment is lower than the β-transus temperature, the Cu and Ni atoms in filler-metal diffuse into the Ti–6Al–4V parent-metal to decrease its β-transus temperature during post-brazing treatment at 880 °C, causing the formation of Widmanstätten structure.

Fig. 9 shows the evolution of the shear strength of joints conducted various post-brazing treatments after brazing at

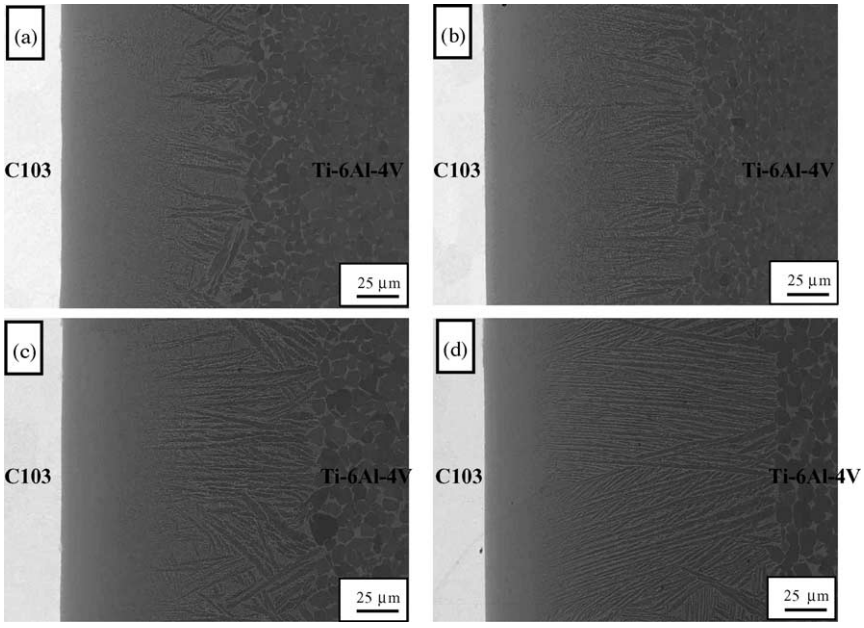

Fig. 8. The microstructure of the C103/TiCuNi/Ti–6Al–4V joint after post-brazing treatment at 880 °C for: (a) 0 h, (b) 2 h, (c) 4 h and (d) 6 h, which was preceded by brazing at 960 °C for 15 min, showing fine, acicular Widmanstätten structure throughout the joint.

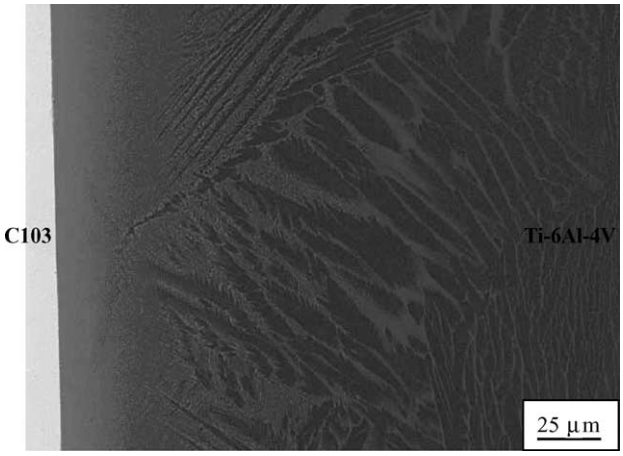

Fig. 10. The microstructure of the C103/TiCuNi/Ti–6Al–4V joint brazed at 1050 °C for 15 min, showing the coarse Widmanstätten structure which deteriorates the joint shear strength.

960 °C for 15 min, indicating that post-brazing treatment at 880 °C for 2 h does not markedly improve the joint strength, because of the short period of heat treatment. However, when the time of post-brazing treatment is prolonged to 4 h, the joint shear strength increases by 16% from 354 to 411 MPa, because the hypoeutectic structure disappears and is displaced by a fine hypereutectoid structure, and no coarse Widmanstätten structure forms in the joint interface.

As mentioned in our previous study [24], if the total Ni amount (Ni plus Cu contents) in the joint interface can be reduced to below 12 wt.% by the isothermal diffusion or the dilution of parent-metals, then the hypoeutectic structure does not form in the joint interface and is replaced by a fine hypereutectoid structure, improving the joint shear strength. Although increasing the brazing temperature can enhance the diffusion of Cu and Ni atoms, changing the hypoeutectic structure into the fine hypereutectoid structure, the coarse acicular Widmanstätten structure is formed in the joint interface and reduces the joint strength, as shown in Fig. 10, because the brazing temperature exceeds the β-transus temperature.

After post-brazing treatment, the Widmanstätten structure still forms in the joint interface, but such a Widmanstätten structure is finer than that caused by the over-high brazing temperature. The fine, non-coarse, Widmanstätten structure in the joint does not seem to affect detrimentally the joint shear strength [11–13]. When the post-brazing treatment is further extended to 6 h, the joint shear strength declines to 299 MPa, because the overlong Widmanstätten structure of nearly 150 μm may reduce the joint shear strength, as shown in Fig. 8(d).

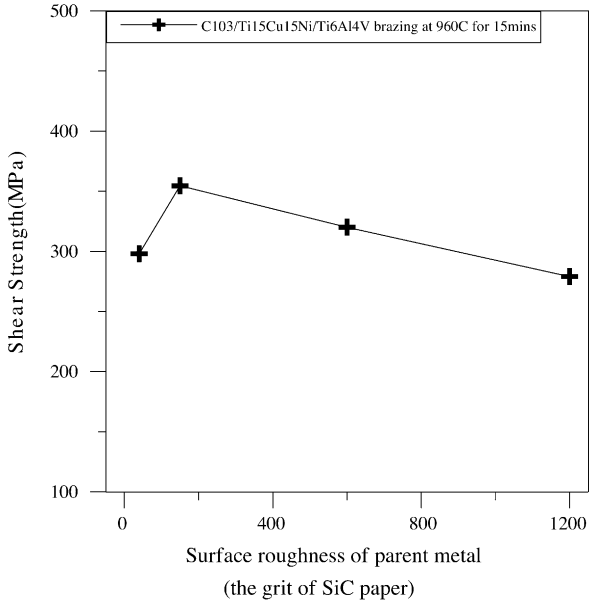

Grit of SiC paper	40	100	600	1200
the surface roughness of C103 (μm Ra)	1.67	0.79	0.09	0.071
the surface roughness of Ti-6Al-4V(μm Ra)	1.58	0.71	0.06	0.054

Fig. 11. Correlation diagram between shear strength and surface roughness of parent-metals of the C103/TiCuNi/Ti–6Al–4V joint brazed at 960 °C for 15 min.

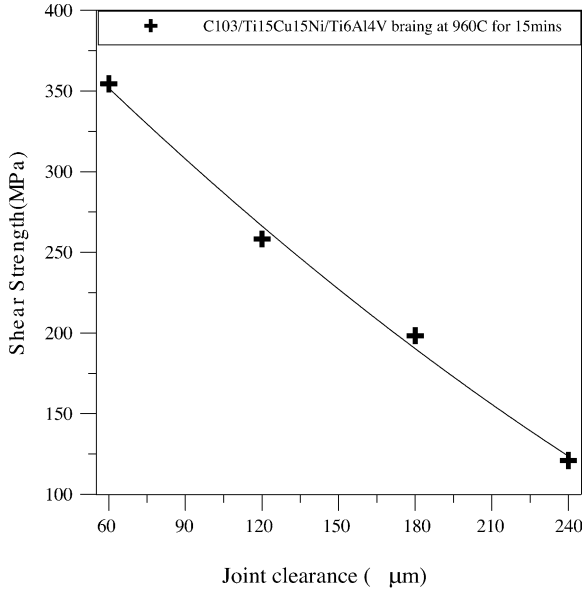

Joint clearance(μm)	60	120	180	240
Fracture mode	II	I	I	I
Shear strength (MPa)	354	258	198	121

Fig. 12. Correlation diagram between shear strength and the joint clearance of the C103/TiCuNi/Ti–6Al–4V joint.

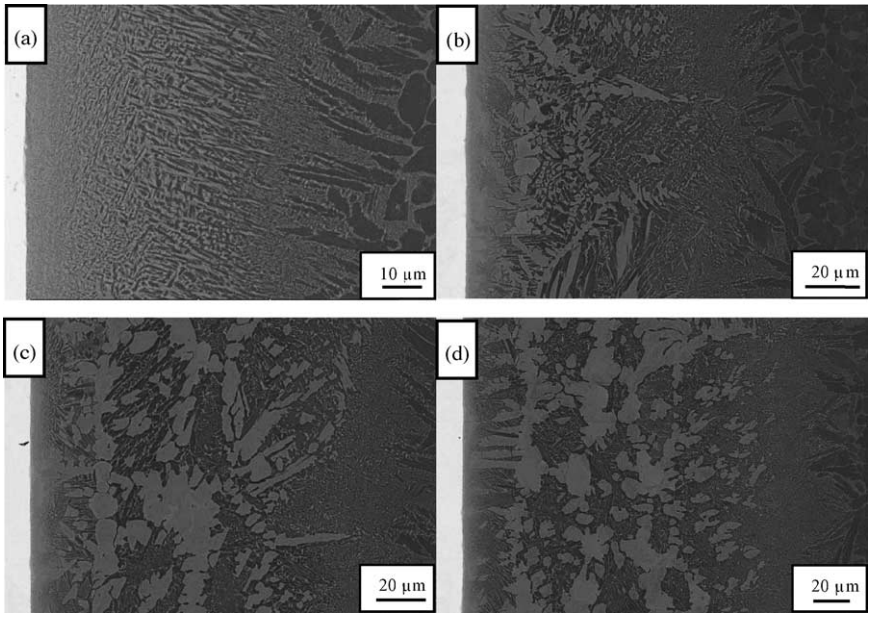

Fig. 13. The microstructure of the C103/TiCuNi/Ti–6Al–4V joint with different joint clearance: (a) 60 μm, (b) 120 μm, (c) 180 μm and (d) 240 μm.

3.5. Surface roughness investigation of C103/TiCuNi/Ti–6Al–4V joint

As the filler-metal melts into liquid, the liquid filler-metal wets the parent-metals and flows through the joint. The surface roughness of parent-metals is an important factor that determines the ease of flow and the wetting of the liquid filler-metal. In general, molten liquid filler-metal can wet a rough surface more effectively than wetting a smooth surface, because a rough surface can change the flow mold of the liquid filler-metal from laminar to turbulent, improving the interaction between the filler-metal and the parent-metals [4].

Fig. 11 plots shear strength of the C103/TiCuNi/Ti–6Al–4V joint versus the surface roughness of the parent-metals. The experimental results in Fig. 11 indicate that

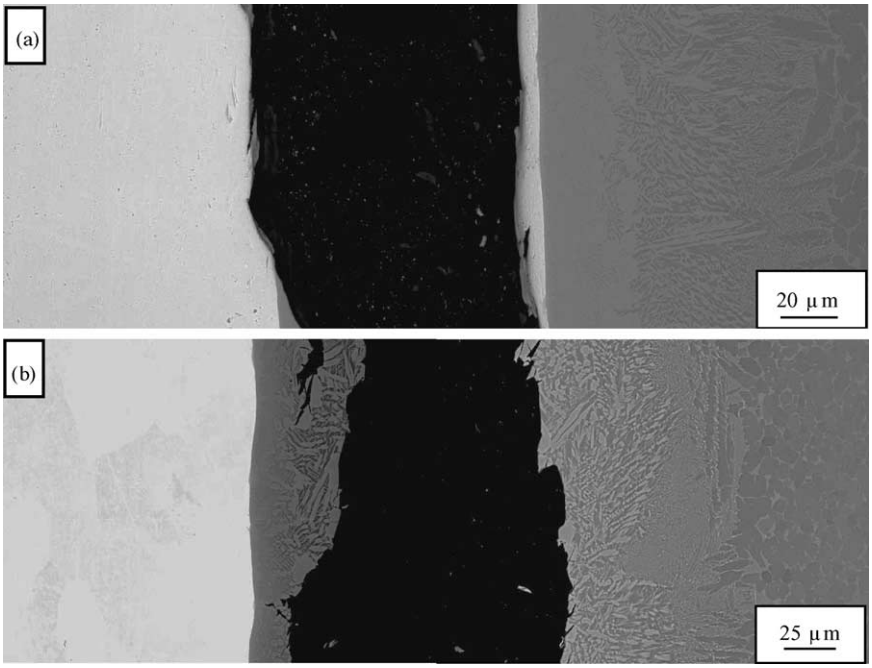

Fig. 14. The cross-section of C103/TiCuNI/Ti–6Al–4V joint with joint clearance of: (a) 60 μm and (b) 120 μm after shear test brazed at 960 °C for 15 min, showing the mode II fracture and the mode I fracture, respectively.

the joint shear strength increases from 298 to 354 MPa as the surface roughness of the C103 parent-metal decreases from 1.67 to 0.79 μm. However, further reducing the surface roughness of the parent-metals reduces the joint strength to 281 MPa. As shown in Fig. 11, if the surface of the parent-metals is too rough, only the steep points on the parent-metals surface can be effectively brazed, causing low joint strength. However, if the surface of the parent-metals is too smooth, then the liquid filler-metal cannot effectively wet and flow throughout the entire joint and may form voids in the joint interface, also causing low joint strength. For the C103/TiCuNi/Ti–6Al–4V joint, before joining, the parent-metals with a surface roughness around 0.7–0.8 μm, polished by SiC paper of 100 grit, is the optimized condition for achieving the maximum shear strength of the joint.

3.6. Joint clearance investigation of C103/TiCuNi/Ti–6Al–4V joint

An appropriate clearance for a brazed joint depends not only on the properties of filler-metal, but also on the surface roughness of parent-metals, the interaction between the parent-metals and the filler-metal, and the brazing process [4]. Fig. 12 plots the relation between the joint clearance and the shear strength of the C103/TiCuNi/Ti–6Al–4V joint, indicating that the shear strength of the joint declines as the joint clearance increases. A joint clearance of 60 μm can achieve the maximum shear strength because a smaller joint clearance increases capillarity and thus the distribution of the filler-metal throughout the joint area, and reduces the formation of voids or shrinkage cavities in the joint as the filler-metal solidifies.

Moreover, the amount of continuous intermetallic-layer in the joint interface increases with the increasing of joint clearance, as shown in Fig. 13. The continuous intermetallic-layer, which consists of brittle intermetallic compounds, causes the decreasing of shear strength. Besides, as the joint clearance increases from 60 to 120 μm or more, the failure mode of the joint changes from mode II to mode I, as shown in Fig. 14.

4. Conclusion

1. Microstructural observations reveal that the microstructure in the joint interface can be divided into seven characteristic zones and each zone has its own chemical composition. The morphology of each zone changes with the brazing time and the brazing temperature.
2. The C103/TiCuNi/Ti–6Al–4V joint brazed at 960 °C for 15 min has the maximum shear strength, 354 MPa. Further increasing the brazing time to 20 min reduces the joint shear strength. Moreover, the shear strength of the C103/TiCuNi/Ti–6Al–4V joint can be maintained at around 300 MPa at a temperature below 600 °C. As the temperature exceeds 600 °C, the shear strength of the joint markedly declines.
3. The fracture load of joint raises with the increasing of the overlap-length. The critical overlap-length of the C103/TiCuNi/Ti–6Al–4V joint is around 3.2. However, the joint shear strength decreases with the increasing of the overlap-length because of the non-uniform stress distribution during shear test.
4. Three sorts of failure modes can be observed in the fracture surface of the C103/TiCuNi/Ti–6Al–4V joints. The failure mode of the joint depends not only on the phases in the joint interface, but also on the joint designs, such as the joint clearance. The joints fractured in mode III have the lower shear strength, whereas those fractured in mode II have the higher shear strength.
5. Post-brazing treatment at 880 °C for 4 h increases the shear strength of the C103/TiCuNi/Ti–6Al–4V joint by 16%, from 354 to 411 MPa. The fine, acicular Widmanstätten structure does not seem to reduce the shear strength.

Acknowledgements

The authors gratefully acknowledge the financial support of this research by National Science Council (NSC), Republic of China, under the grants NSC 92-2623-7-014-012.

References

[1] W.F. Smith, Structure and Properties of Engineering Alloys, McGraw-Hill Inc., 1993.
[2] J.R. Davis, Metals Handbook, Properties and Selection: Nonferrous Alloys and Special Purpose Materials, vol. 2, ASM International, 1990.
[3] R. Roger, E.W. Collings, G. Welsch, Materials Properties Handbook: Titanium Alloys, ASM International, Materials Park, 1993.
[4] J.R. Davis, K. Ferjutz, N.D. Wheaton, Metals Handbook; Welding, Brazing, and Soldering, vol. 6, ASM International, 1990.
[5] J.J. Stephens, JOM. 8 (1990) 22.
[6] T.B. Massalski, Binary Alloy Phase Diagrams, ASM International, Materials Park, 1990.
[7] P. Villars, A. Prince, H. Okamoto, Handbook of Ternary Alloy Phase Diagrams, ASM, International, Materials Park, OH, 1995.
[8] H.Y. Chan, D.W. Liaw, R.K. Shiue, Mater. Lett. 58 (2004) 1141.
[9] H.Y. Chan, D.W. Liaw, R.K. Shiue, Int. J. Refractory Met. Hard Mater. 22 (2004) 27.
[11] O. Botstein, A. Schwarzman, A. Rabinkin, Mater. Sci. Eng. A 206 (1995) 14.
[12] A. Hirose, M. Nojiri, H. Ito, K.F. Kobayashi, Int. J. Mater. Prod. Technol. 13 (1998) 13.
[13] O. Botstein, A. Rabinkin, Mater. Sci. Eng. A188 (1994) 305.
[14] T.J. Moore, Weld. Res. Suppl. (March) (1990) 98.
[15] G.K. Watson, T.J. Moore, Weld. J. 56 (1977) 306.
[16] S.J. Lee, S.K. Wu, R.Y. Lin, Acta Mater. 46 (1998) 1283.
[17] S.J. Lee, S.K. Wu, R.Y. Lin, Acta Mater. 46 (1998) 1297.
[18] R. Hill, E. Robert, Physical Metallurgy Principles, PWS-Kent Pub., Boston, 1992.
[19] S.W. Lan, Weld. J. 10 (1982) 23.

[20] T. Onzawa, A. Suzumura, M.W. Ko, Weld. Res. Suppl. 10 (1990) 462.
[21] X.P. Zhang, Y.W. Shi, Scripta Mater. 50 (2004) 1003.
[23] A. Rabinkin, H. Liebermann, S. Pounds, T. Taylor, Scripta Metallurgica et Materialia 25 (1991) 399.
[24] I.-T. Hong, C.-H. Koo, Mater. Sci. Eng. A 398 (2005) 113.
[25] N. Bredzs, F.M. Miller, Weld. J. 11 (1968) 481.
[26] E. Lugscheider, H. Reimann, O. Knotek, Weld. J. 6 (1997) 189.
[27] Y. Flom, L. Wang, Weld. J. 7 (2004) 32.
[28] C.W. Shaw, L.A. Shepard, J. Wulff, Trans. ASM 57 (1964) 94.